Pramana, Vol. 19, No. 2, August 1982, pp. 141–150. © Printed in India.

# Motion of the charged particles off the equatorial plane of a Kerr black hole in an electromagnetic field

D K CHAKRABORTY* and A R PRASANNA
Physical Research Laboratory, Ahmedabad 380 009, India
*Permanent address: Government College, Jagdalpur 494 005, India

MS received 31 December 1981; revised 1 June 1982

**Abstract.** Charged particle orbits off the equatorial plane of a Kerr black hole in an external electromagnetic field is studied, both for dipole as well as uniform magnetic field. Particles are found to get trapped by the magnetic field if the initial value of the parallel velocity is small. Bending of the field lines in the vicinity of the hole and the consequent trapping of the particles in an otherwise uniform magnetic field indicates the significance of general relativistic effects in such cases.

**Keywords.** Charged particle orbits; general relativity; motion along the field lines.

Plasma processes around compact objects like neutron stars and black holes are generally considered to be the main mechanism of the radiation from high energy source like quasars, x-ray binaries and the like. Studies of charged particle orbits in electromagnetic fields around those compact objects provide one of the ways of studying the plasma dynamics in these situations. Particle orbits in external electromagnetic field on Schwarzschild and Kerr geometry have been studied by Prasanna and Varma (1977) and Prasanna and Vishveshwara (1978). From the studies of equatorial orbits they found that stable orbits exist even very close to the event horizon. Following this result Prasanna and Chakraborty (1981) investigated the stability of the infinitesimally thin rotating charged fluid disks around a Schwarzschild black hole whose inner edge is very near to the event horizon (very much inside 6m, $m = MG/c^2$) and found that such disks are generally stable. It might be possible to get some information regarding the thickness of a thick stable disk from studies of trapped orbits of the charged particle off the equatorial plane.

To study the motion of the charged particles off the equatorial plane of a Kerr black hole we first study the structure of the electromagnetic field in a more detailed way. The four potential $A_i$ as given by Petterson (1975) for a dipole magnetic field and by Wald (1974) for a uniform magnetic field are given by (using the same notations as of Prasanna and Vishveshwara 1978)

Case (i) dipolar field:

$$A_T = -\frac{3a\lambda}{2\Sigma(1-a^2)}\left[\{\rho(\rho-1)-(a^2-\rho)\cos^2\theta\}\frac{1}{2(1-a^2)^{1/2}}\right.$$

$$\ln\left\{\frac{\rho-1+(1-a^2)^{1/2}}{\rho-1-(1-a^2)^{1/2}}\right\}-(\rho-\cos^2\theta)\Bigg] \tag{1}$$

$$\bar{A}_\varphi=-\frac{3\lambda\sin^2\theta}{4\Sigma(1-a^2)}\Bigg[-\{\rho(\rho^3+a^2\rho-2a^2)+\Delta a^2\cos^2\theta\}\frac{1}{2(1-a^2)^{1/2}}$$

$$\ln\left\{\frac{\rho-1+(1-a^2)^{1/2}}{\rho-1-(1-a^2)^{1/2}}\right\}+(\rho-1)a^2\cos^2\theta+\rho(\rho^2+\rho+2a^2)\Bigg]. \tag{2}$$

Case (ii) uniform field:

$$A_T=-a\lambda\left[1-\frac{\rho}{\Sigma}(2-\sin^2\theta)\right] \tag{3}$$

$$\bar{A}_\varphi=\frac{\lambda\sin^2\theta}{2\Sigma}[(\rho^2+a^2)^2-\Delta a^2\sin^2\theta-4a^2\rho]. \tag{4}$$

From these we construct the field tensor given by

$$F_{ij}=A_{j,i}-A_{i,j} \tag{5}$$

and transform them to locally nonrotating frame (LNRF) using the law of transformation

$$F^{(i)}{}_{(j)}=e^{(i)}{}_l\, e_{(j)}{}^m\, F^l{}_m \tag{6}$$

where the transformation matrix $e^{(i)}{}_j$ is given by

$$e^{(i)}{}_j=\begin{bmatrix}(\Sigma\Delta/B)^{1/2} & 0 & 0 & 0\\ 0 & (\Sigma/\Delta)^{1/2} & 0 & 0\\ 0 & 0 & \Sigma^{1/2} & 0\\ -\dfrac{2a\rho}{\Sigma^{1/2}B^{1/2}}\sin\theta & 0 & 0 & \left(\dfrac{B}{\Sigma}\right)^{1/2}\sin\theta\end{bmatrix} \tag{7}$$

and $e^l_{(j)}$ is its inverse. The components of electric field ($E_r$, $E_\theta$, $E_\varphi$) and of the magnetic field ($B_r$, $B_\theta$, $B_\varphi$) in LNRF are then given by

$$\bar{E}_r=\frac{B^{1/2}}{\Sigma}A_{T,\rho}+\frac{2a\rho}{\Sigma B^{1/2}}\bar{A}_{\varphi,\rho}$$

$$\bar{E}_\theta = \left(\frac{B}{\Delta}\right)^{1/2} \frac{1}{\Sigma} A_{\tau,\theta} + \frac{2\alpha\rho}{\Sigma(\Delta B)^{1/2}} \bar{A}_{\varphi,\theta}$$

$$\bar{E}_\varphi = 0$$

$$\bar{B}_r = \frac{1}{B^{1/2}\sin\theta} \bar{A}_{\varphi,\theta}$$

$$\bar{B}_\theta = -\left(\frac{\Delta}{B}\right)^{1/2} \frac{\bar{A}_{\varphi,\rho}}{\sin\theta}$$

$$\bar{B}_\varphi = 0 \tag{8}$$

where $\bar{E}_\mu = m E_\mu$ and $\bar{B}_\mu = m B_\mu$.

We plot the lines of force defined by

$$ds_\mu = K \bar{B}_\mu \tag{9}$$

for magnetic field and

$$ds_\mu = K \bar{E}_\mu \tag{10}$$

for electric field, $K$ being a constant. For specific choices of $\alpha$ and $\lambda$ the plots of lines of force in the meridional plane are presented in figure 1 for the case of the dipolar field and in figure 5 for the case of the uniform field.

We also calculate the components of 3-velocity parallel and perpendicular to the magnetic field lines. The components of the four velocity in LNRF are

$$U^{(\varphi)} = \left(\frac{\Sigma}{\Delta}\right)^{1/2} U^\rho, \quad U^{(\theta)} = \Sigma^{1/2} U^\theta$$

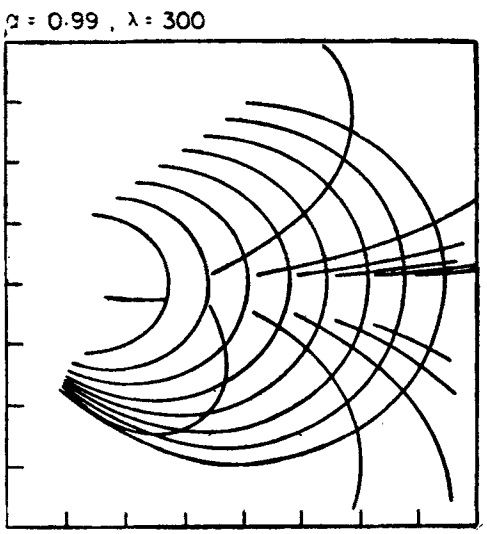


**Figure 1.** Lines of force for magnetic and electric fields for dipole field.

$$U^{(\varphi)} = \left(\frac{B}{\Sigma}\right)^{1/2} \sin\theta\, U^{\varphi} - \frac{2a\rho}{(B\Sigma)^{1/2}} \sin\theta\, U^{\tau}$$

$$U^{(\tau)} = \left(\frac{\Sigma\Delta}{B}\right)^{1/2} U^{\tau} \tag{11}$$

and the components of the 3-velocity $V^{(a)}$ are then (in LNRF)

$$V^{(\rho)} = \frac{cU^{(\rho)}}{U^{(\tau)}}, \quad V^{(\theta)} = \frac{cU^{(\theta)}}{U^{(\tau)}}, \quad V^{(\phi)} = \frac{cU^{(\varphi)}}{U^{(\tau)}} \tag{12}$$

Defining the angle $Z$ between $\bar{B}_r$ and the lines of force by

$$\tan Z = \frac{\bar{B}_\theta}{\bar{B}_r}, \tag{13}$$

we find the parallel and perpendicular components $V_{\|}$ and $V_{\perp}$ of the 3-velocity to be

$$V_{\|} = V^{(\rho)} \cos Z + V^{(\theta)} \sin Z$$

$$V_{\perp} = \{V^{(\varphi)^2} + (V^{(\rho)} \sin Z - V^{(\theta)} \cos Z)^2\}^{1/2} \tag{14}$$

Actual orbits of the particles are obtained by integrating numerically the equations of motion (19) to (22) of Prasanna and Vishveshwara along with the field components (1) to (4). Along its trajectory we also calculate $V_{\|}$ and $V_{\perp}$. To fix up the initial conditions we note that when $\theta = \pi/2$ and $U^{\theta} = 0$

$$(U^{\rho})^2 \equiv (U^{\rho})^2_{0,\pi/2} = \frac{1}{\rho^3}[\{\rho(\rho^2 + a^2) + 2a^2\}(E + A_{\tau})^2$$

$$-4a(E + A_{\tau})(L - \bar{A}_{\varphi}) - (\rho - 2)(L - \bar{A}_{\varphi})^2 - \rho\Delta]. \tag{15}$$

Putting $U^{\rho} = 0$ in the above one obtains the effective potential $V_{\text{eff}}$ for the motion of the particle confined to $\theta = \pi/2$ plane. For a selected value of energy $E$ this $V_{\text{eff}}$ curve gives turning points $\rho_1$ and $\rho_2$ such that for any $\rho$ satisfying $\rho_1 < \rho < \rho_2$ as calculated from (15) is real. Now if we take $\theta = \pi/2$ but $U^{\theta} \neq 0$, the normalisation condition for the four velocity yields

$$(U^{\rho})^2 = (U^{\rho})^2_{0,\pi/2} - \Delta(U^{\theta})^2. \tag{16}$$

Since $\Delta$ is positive for any $\rho$ outside the event horizon, $U^{\rho}$ as given by (16) is real for the same $E$ as above and for $\rho$ satisfying $\rho_1 < \rho < \rho_2$ when

$$0 < \Delta(U^{\theta})^2 < (U^{\rho})^2_{0,\pi/2} \tag{17}$$

This sets the upper bound for $U^\theta$. We fix up the initial positions (denoted by subscript '0') $\varphi_0 = 0$, $\theta_0 = \pi/2$, $\rho_1 < \rho_0 < \rho_2$ and calculate the maximum allowed $U^\theta$ at the initial position, as given by the inequality (17). Using any value of $U^\theta$ between the maximum and zero as its initial value we calculate the initial $U^\rho$ by using (16).

Tables 1 to 4 show the values of $\rho$, $\theta$, $\varphi$, $V_{\|}$ and $\bar{B}$ where $\bar{B}$ is the net magnetic

**Table 1.** Orbits of the particles in $(\rho - \theta)$ plane showing $\rho$, $\theta$, $\varphi$, $V_{\|}$ and $\bar{B}$ for dipole and uniform fields.
$\alpha = 0{\cdot}45$, $\lambda = 300$, $L = 100$, $E = 5$, $V_{\|_0} = 0{\cdot}78$ dipole field.

| $\rho$ | $\theta$ | $\varphi$ | $V_{\|}$ | $\bar{B}$ |
|---|---|---|---|---|
| 4·56 | 1·57 | 0·0 | 0·78 | 5·45 |
| 4·31 | 1·20 | −0·016 | 0·92 | 6·82 |
| 4·26 | 1·84 | −0·047 | 0·84 | 7·51 |
| 4·32 | 2·00 | −0·005 | 0·63 | 7·70 |
| 4·25 | 2·10 | 0·15 | 0·50 | 8·65 |
| 3·88 | 2·11 | 0·31 | 0·45 | 12·24 |
| 3·48 | 2·11 | 0·22 | 0·54 | 18·62 |
| 3·51 | 2·31 | 0·25 | 0·40 | 19·84 |
| 3·22 | 2·27 | 0·46 | 0·46 | 27·55 |
| 3·08 | 2·26 | 0·35 | 0·53 | 32·86 |
| 3·04 | 2·34 | 0·33 | 0·54 | 35·55 |
| 3·01 | 2·45 | 0.43 | 0.54 | 38.75 |
| 2·82 | 2·44 | 0·61 | 0·65 | 51·11 |
| 2·58 | 2·48 | 0·51 | 0·75 | 77·15 |
| 2·34 | 2·65 | 0·78 | 0·85 | 131·0 |
| 2·22 | 2·64 | 0·85 | 0·53 | 182·4 |
| 2·11 | 2·68 | 0·85 | 0·96 | 251·8 |

**Table 2.** Orbits of the particles in $(\rho - \theta)$ plane showing $\rho$, $\theta$, $\varphi$, $V_{\|}$ and $\bar{B}$ for dipole and uniform fields.
$\alpha = 0{\cdot}45$, $\lambda = 300$, $L = 100$, $E = 5$, $V_{\|_0} = 0{\cdot}15$ dipole field.

| $\rho$ | $\theta$ | $\varphi$ | $V_{\|}$ | $\bar{B}$ |
|---|---|---|---|---|
| 4·56 | 1·57 | 0·0 | 0·15 | 5·49 |
| 4·31 | 1·68 | −0·21 | 0·21 | 6·82 |
| 4·57 | 1·75 | −0·15 | 0·03 | 4·11 |
| 5·31 | 1·78 | −0·04 | −0·04 | 3·31 |
| 5·14 | 1·67 | 0·52 | −0·33 | 3·57 |
| 4·15 | 1·42 | 0·54 | −0·75 | 7·96 |
| 4·31 | 1·11 | 0·88 | −0·14 | 7·96 |
| 4·24 | 1·13 | 0·76 | 0·14 | 2·37 |
| 4·19 | 1·46 | 1·13 | 0·79 | 7·56 |
| 5·25 | 1·77 | 1·24 | 0·26 | 3·41 |
| 5·12 | 1·82 | 1·70 | 0·01 | 3·80 |
| 4·54 | 1·74 | 1·83 | −0·15 | 5·74 |
| 5·35 | 1·54 | 1·76 | −0·12 | 2·55 |
| 5·62 | 1·50 | 2·37 | −0·001 | 2·60 |
| 4·42 | 1·54 | 2·60 | 0·05 | 6·10 |
| 4·05 | 1·57 | 2·45 | 0·13 | 8·24 |
| 5·33 | 1·62 | 2·50 | 0·02 | 3·11 |
| 5·87 | 1·63 | 2·86 | −0·03 | 2·23 |
| 5·03 | 1·58 | 3·31 | −0·13 | 3·83 |

**Table 3.** Orbits of the particles in $(\rho - \theta)$ plane showing $\rho$, $\theta$, $\varphi$, $V_{\|}$ and $B$ for dipole and uniform fields.
$a = 0{\cdot}45$, $\lambda = 50$, $L = 1000$, $E = 25{\cdot}0$, $V_{\|0} = 0{\cdot}27$, uniform field

| $\rho$ | $\theta$ | $\varphi$ | $V_{\|}$ | $\bar{B}$ |
|---|---|---|---|---|
| 6·31 | 1·57 | 0·0 | −0·27 | 41·36 |
| 6·34 | 1·60 | 0·055 | −0·27 | 41·43 |
| 6·38 | 1·61 | 0·007 | −0·27 | 41·34 |
| 6·21 | 1·68 | 0·035 | −0·27 | 41·34 |
| 6·45 | 1·71 | 0·016 | −0·27 | 41·75 |
| 6·47 | 1·74 | 0·084 | −0·27 | 41·86 |
| 6·36 | 1·78 | 0·063 | −0·27 | 41·85 |
| 6·56 | 1·80 | 0·024 | −0·27 | 42·18 |
| 6·76 | 1·87 | 0·045 | −0·26 | 42·75 |
| 6·74 | 1·95 | 0·088 | −0·25 | 43·14 |
| 6·85 | 1·96 | 0·085 | −0·25 | 44·34 |
| 6·85 | 2·02 | 0·084 | −0·24 | 43·78 |
| 7·09 | 2·04 | 0·054 | −0·23 | 44·08 |
| 7·30 | 2·07 | 0·052 | −0·20 | 44·45 |
| 7·55 | 2·13 | 0·101 | −0·15 | 44·55 |

**Table 4.** Orbits of the particles in $(\rho - \theta)$ plane showing $\rho$, $\theta$, $\varphi$, $V_{\|}$ and $\bar{B}$ for dipole and uniform fields.
$a = 0{\cdot}45$, $\lambda = 50$, $L = 1000$, $E = 25{\cdot}0$, $V_{\|0} = 0{\cdot}18$, uniform field

| $\rho$ | $\theta$ | $\varphi$ | $V_{\|}$ | $\bar{B}$ |
|---|---|---|---|---|
| 6·31 | 1·57 | 0·0 | −0·16 | 41·38 |
| 6·45 | 1·65 | 0·054 | −0·18 | 41·64 |
| 6·44 | 1·77 | 0·079 | −0·18 | 41·80 |
| 6·46 | 1·86 | 0·074 | −0·17 | 42·34 |
| 6·70 | 1·93 | 0·046 | −0·16 | 42·98 |
| 6·91 | 2·03 | 0·075 | −0·11 | 43·83 |
| 7·01 | 2·07 | 0·097 | −0·06 | 44·17 |
| 7·09 | 2·08 | 0·103 | $-0{\cdot}6 \times 10^{-4}$ | 44·33 |
| 7·09 | 2·08 | 0·126 | $0{\cdot}3 \times 10^{-3}$ | 44·33 |
| 7·02 | 2·05 | 0·109 | 0·077 | 44·05 |
| 7·01 | 1·97 | 0·146 | 0·14 | 43·56 |
| 6·66 | 1·88 | 0·132 | 0·17 | 42·70 |
| 6·32 | 1·77 | 0·159 | 0·18 | 41·78 |
| 6·36 | 1·63 | 0·217 | 0·18 | 41·49 |
| 6·33 | 1·57 | 0·225 | 0·18 | 41·41 |

field along the trajectory of the particle for dipolar field (tables 1 and 2) and for uniform field (tables 3 and 4). It is seen from these tables that for the same values of $a$, $\lambda$, $E$ and $L$ particles get reflected from a point (mirror point) lying off the equatorial plane when the initial value of $V_{\|}$ $(= V_{\|0})$ is small. $V_{\|}$ changes sign on each reflection (tables 2 and 4). In case $V_{\|0}$ is too high, the particle continues to proceed towards the event horizon in dipolar field (table 1) or escapes to infinity in uniform field (table 3) without showing any sign of reflection.

Figure 1 shows the structure of magnetic and electric lines of force for the specific values of $\alpha$ and $\lambda$ for the case of dipolar field. Taking the same $\alpha$ and $\lambda$ and specific values of $E$, $L$ and $\rho_0$, plots of actual orbits of the particle are presented through figures 2-4 with different choices of $V_{\|0}$. We find that particles, more or less follow the magnetic field lines and get trapped between the mirror points provided $V_{\|0}$ is small.

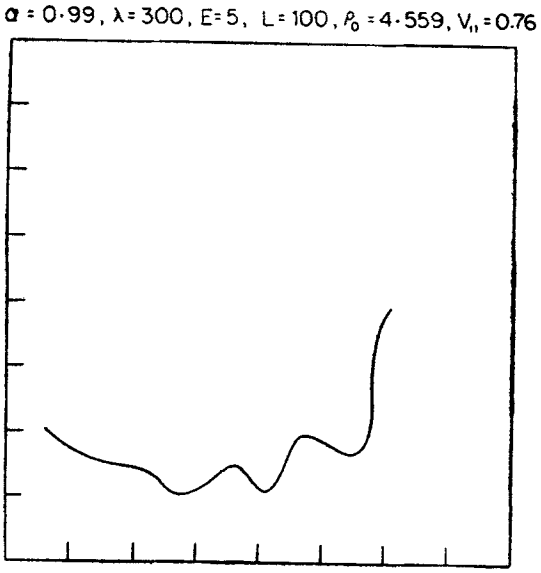


**Figure 2.**

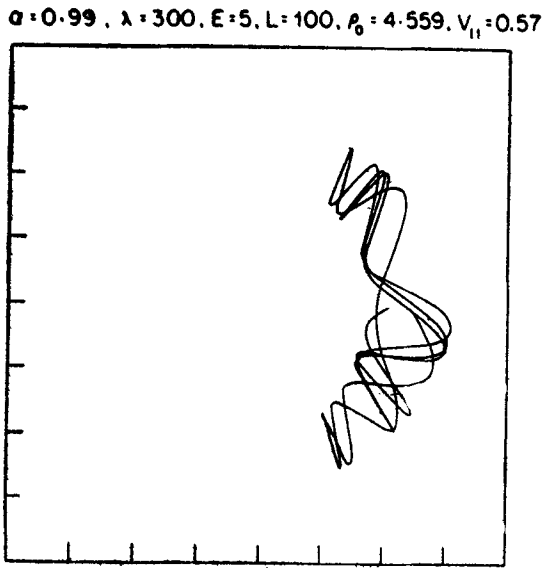


**Figure 3.**

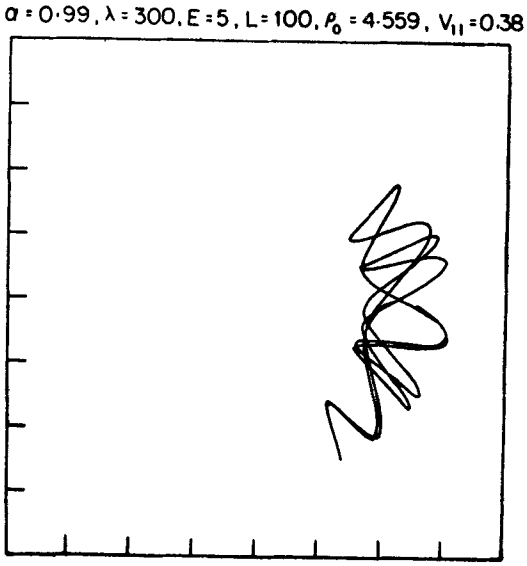


**Figure 4.**

**Figures 2-4.** Orbits of the particles off the equatorial plane for dipole field.

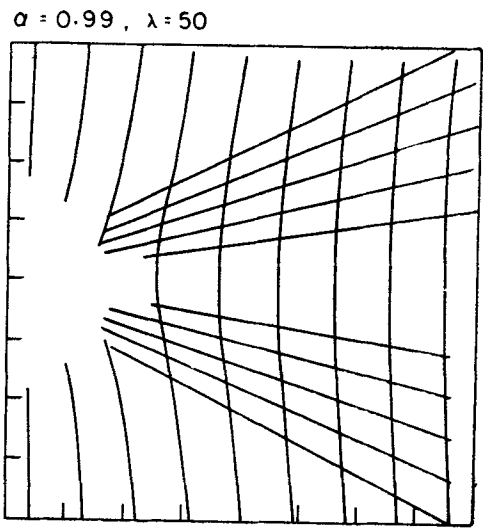


**Figure 5.** Same as figure 1 for uniform field.

For the case of uniform field figure 5 shows the structure of magnetic and electric lines of force for specific choices of $\alpha$ and $\lambda$ while figures 6–8 show few cases of trapped orbits, for the same $\alpha$ and $\lambda$ as in figure 5, for a fixed value of $E$ and for different values of $L$, $\rho_0$ and $V_{\|0}$.

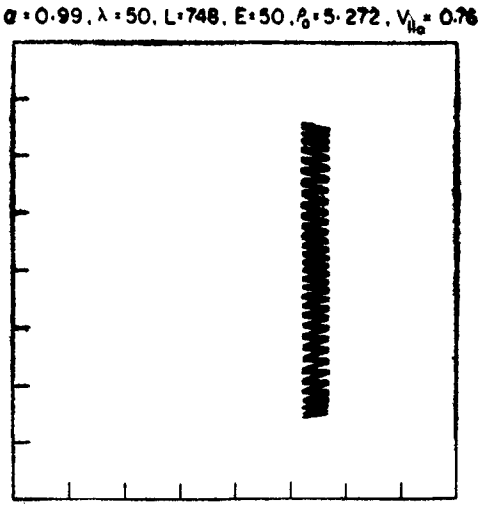


Figure 6.

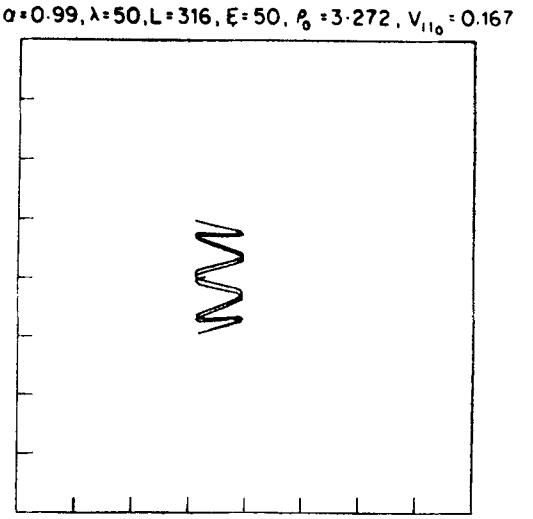


Figure 7.

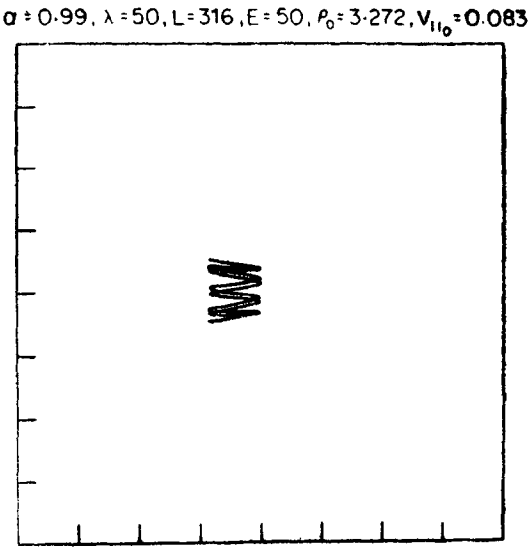


Figure 8.

**Figures 6-8.** Same as figures 2-4 for uniform field.

## Discussion and Conclusions

In the above analysis we have considered the motion of charged particles off the equatorial plane in dipolar and uniform magnetic fields superposed on Kerr geometry. Depending on the field strengths and initial velocity the particles either get trapped in orbits which exhibit reflection at mirror points or move continuously towards the black hole in dipole field, or escape to infinity in uniform magnetic field. From the structure of field lines it is clear that in dipole field the field strengths increase towards the pole, whereas in uniform field the field strength first increases at points away from the poles but off the equatorial plane, and then becomes constant at a large distance from the Kerr black hole. In dipole field the trajectories are more or less similar to what one has in the nonrelativistic case whereas in uniform field the bending of field lines is essentially a general relativistic effect caused entirely by the presence of the black hole. This bending of field lines near the equatorial plane makes plausible the field gradient in an otherwise uniform field, and thus makes trapping possible. Of the number of examples we considered only few showed a possible trapping of which the case $\lambda = 50$, we have presented. This case refers, for a particle of the type of proton, to a magnetic field strength of the order of $10^{-5}$ Gauss, the mass of the black hole to be about $\sim 10^8\ M_\odot$. Thus one can see that this case could model the field deformation in the galactic magnetic field near a supermassive black hole. The existence of trapped orbits with reflection points at different distances off the equatorial plane depending on the initial velocity and position clearly shows the possibility of structured (thick) disks of charged particles forming around a supermassive black hole just due to the galactic magnetic field.

## Acknowledgement

One of us (DKC) would like to thank the UGC for the award of Teacher Fellowship and the Director, Physical Research Laboratory, for local hospitality during his stay at Ahmedabad.

## References

Prasanna A R and Varma R K 1977 *Pramana* **8** 229
Prasanna A R and Vishveshwara C V 1978 *Pramana* **11** 359
Prasanna A R and Chakraborty D K 1981 *J. Astrophys. Astron.* **2** 1
Petterson J A 1975 *Phys. Rev.* D **12** 218
Wald R M 1974 *Phys. Rev.* D **10** 1680